The micro-pulling-down growth of Eu3+-doped Y3Al5O12 and Y3ScAl4O12 crystals for red luminescence

Jie Xu, Qingsong Song, Jian Liu, Kaiting Bian, Wen Lu, Dongzhen Li, Peng Liu, Xiaodong Xu, Yuchong Ding, Jun Xu, et al.

The micro-pulling-down growth of Eu^{3+}-doped $Y_3Al_5O_{12}$ and $Y_3ScAl_4O_{12}$ crystals for red luminescence

Jie Xu[a], Qingsong Song[a], Jian Liu[b], Kaiting Bian[a], Wen Lu[a], Dongzhen Li[a], Peng Liu[a], Xiaodong Xu[a,*], Yuchong Ding[c], Jun Xu[b,*] Kheirreddine Lebbou[d,*]

a Jiangsu Key Laboratory of Advanced Laser Materials and Devices, School of Physics and Electronic Engineering, Jiangsu Normal University, Xuzhou 221116, China
b School of Physics Science and Engineering, Institute for Advanced Study, Tongji University, Shanghai 200092, China
c Research & Development Center of Material and Equipment, China Electronics Technology Group Corporation No.26 Research Institute, Chongqing 400060, China
d Institut Lumière Matière, UMR5306 Université Lyon1-CNRS, Université de Lyon, Lyon 69622, Villeurbanne Cedex, France

Corresponding author:
Email address: xdxu79@jsnu.edu.cn (X. Xu), xujun@mail.shcnc.ac.cn (J. Xu), kheirreddine.lebbou@univ-lyon1.fr (K. Lebbou)

Tel: +86-13916443810

Abstract:
We report on the comparative growth and spectroscopy of Eu^{3+}-doped $Y_3Al_5O_{12}$ (YAG) and $Y_3ScAl_4O_{12}$ crystals grown by the micro-pulling-down (μ-PD) method. The structure of the as-grown crystals was determined by X-ray diffraction (XRD) and Raman spectroscopy. The spectra of the crystals are dominated by a strong line centered at 395 nm, matching well with the emission of commercial ultraviolet laser diodes. The Eu:YAG and Eu:$Y_3ScAl_4O_{12}$ crystals exhibit strongest red emission centered at 710 nm and the full width at half maximum (FWHM) was calculated to be 2.03 and 3.19 nm, respectively. The fluorescence decay curves of $^5D_0$ levels were measured and discussed. All the results indicate that the Eu:YAG and Eu:$Y_3ScAl_4O_{12}$ crystals are promising candidates for red luminescent/laser materials.

Keywords: Eu:YAG; Eu:$Y_3ScAl_4O_{12}$; Micro-pulling-down technique; Spectral property

1. Introduction:

In recent years, the red luminescent materials have attracted much attention because of their potential applications in white light-emitting diodes (W-LEDs), field emission display (FED), vacuum fluorescent displays (VFDs), plasma display panels (PDP) [1-4]. As one of the most popular used red emitting activators, the trivalent europium ion (Eu^{3+}) exhibits characteristic emissions which are associated to the f-f transitions form the excited level $^5D_0$ to lower levels ^7F_J (J=0, 1, 2, 3, 4). Up to now, the Eu^{3+}-doped phosphors, such as Eu:YAG [5], Eu:$Sr_3Bi(PO_4)_3$ [6], Eu:$Ca_9ZnK(PO_4)_7$ [7], Eu:$Na_3Sc_2(PO_4)_3$ [8], and Eu:$Ca_3Y(AlO)_3(BO_3)_4$ [9] have merited considerable attention due to potential applications in red emission. However, it is well known that phosphors have many drawbacks, such as lower uniformity, deficiency of red emission, light scattering and encapsulation difficulty. Therefore, in order to overcome the above disadvantages, search for new red luminescent materials which have better optical properties and chemical stability become an urgent task. The preparation and spectral properties of Eu:YAG ceramics [10], Eu:$Gd_3Sc_2Ga_3O_{12}$ nanocrystalline [11], Eu:$CaGdAlO_4$ crystal [12], Eu:$YAl_3(BO_3)_4$ crystal [13], Er:$KGd(WO_4)_2$ crystal [14] and Eu:$Bi_4Ge_3O_{12}$ crystal [15] have been reported for exploring new luminescent/laser materials.

$Y_3ScAl_4O_{12}$ belongs to the disordered material in which the Sc^{3+} and Al^{3+} ions randomly occupy the same lattice site, which leads to inhomogeneous broadening of absorption and emission spectra [16-19]. $Y_3ScAl_4O_{12}$ has been realized as a valuable material thanks to its high optical, excellent chemical and mechanical characteristics. To the best of our knowledge and in spite of the possibilities to crystalize this material from the melt, up to now there has no research about the growth and performance of Eu:$Y_3ScAl_4O_{12}$ crystal.

In this paper, we select to study two Eu^{3+}-doped garnet hosts (YAG and $Y_3ScAl_4O_{12}$). They crystallize in Ia3d of the cubic crystal system. In these two materials, Y^{3+} and Al^{3+} can be substituted by different types of cations with different sizes and valences up to certain concentration. In this work, attention was focused to grow Eu^{3+}-doped YAG and $Y_3ScAl_4O_{12}$ crystals were by the micro-pulling-down (μ-PD) technique for the first time. The structure of two crystals were studied by X-ray diffraction (XRD). The spectroscopic properties of two crystals were also investigated.

2. Experimental

The Eu^{3+}-doped YAG and $Y_3ScAl_4O_{12}$ single crystals were grown by the μ-PD method [20-23]. The Eu_2O_3, Sc_2O_3, Y_2O_3 and Al_2O_3 powders with high purity of 99.999% were used as raw materials. The starting materials were weighed according to the formula $(Eu_{0.02}Y_{0.98})_3Al_5O_{12}$, $(Eu_{0.02}Y_{0.98})_3ScAl_4O_{12}$, respectively, and then ground and mixed thoroughly in an agate mortar. The mixtures were shaped into a rod and pressed by cold isostatic at 160 MPa for 2 min, then sintered at 1300 ℃ for 20 h in air. A <111> oriented YAG crystal was used as seed, the pulling rate was 0.3 mm/min and the growth atmosphere was high-purity flowing argon. A small portion of as-grown crystals were ground into powders and the powders were carried out in the 2θ range of 20°–90° by X-ray diffraction method (XRD, Bruker-D2, Germany) at room temperature. The Raman spectra were obtained with a laser Raman spectrometer (Omni-λ 300i, Zolix) in the range of 16-900 cm^{-1} at 30 MV with a 785 nm excitation light source. The absorption spectra of Eu:YAG and Eu:$Y_3ScAl_4O_{12}$ crystals

were recorded with a UV–VIS–NIR spectrophotometer (Lambda 900, Perkin -Elmer UV-VIS-NIR) in the range of 300-450 nm. The fluorescence spectra, as well as the lifetime were recorded using Edinburgh Instruments FLS980 spectrophotometer under 394 nm excitation. All the measurements were taken at room temperature. The samples were cut from the as-grown crystals and two surfaces perpendicular to the <111>-growth axis was polished for spectral measurements. The spectral measurements were detected in the core (diameter of 0.5 mm) of the samples.

3. Results and discussions

3.1 Crystal growth

After growth the crystals were cooled to room temperature during 3 h. As shown in Fig. 1, as-grown Eu:YAG and Eu:$Y_3ScAl_4O_{12}$ crystals with diameter of about 2 mm were crystallized. We obtain blue transparent Eu^{3+}-doped YAG crystal (Fig.1a) and slightly dark brown Eu^{3+}-doped $Y_3ScAl_4O_{12}$ crystal (Fig.1b), with homogeneous diameter and free of macroscopic defects. During the growth process, the melt meniscus thickness under the capillary die did not exceed 250 μm, it is considered a good value for a stable growth. The length of the grown fibers reached 10 cm while 100% of the melt in the crucible was crystallized. We did not record any macro-scale shift from the <111> initial orientation.

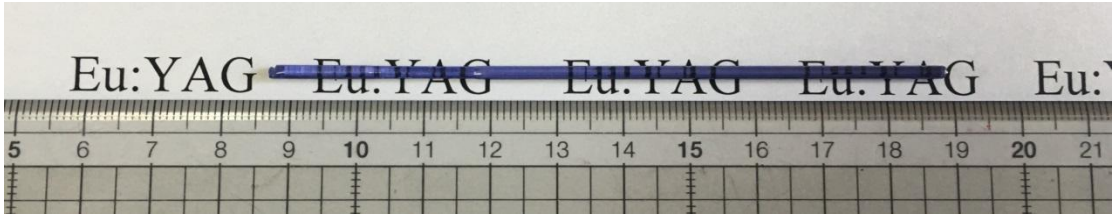

(a)

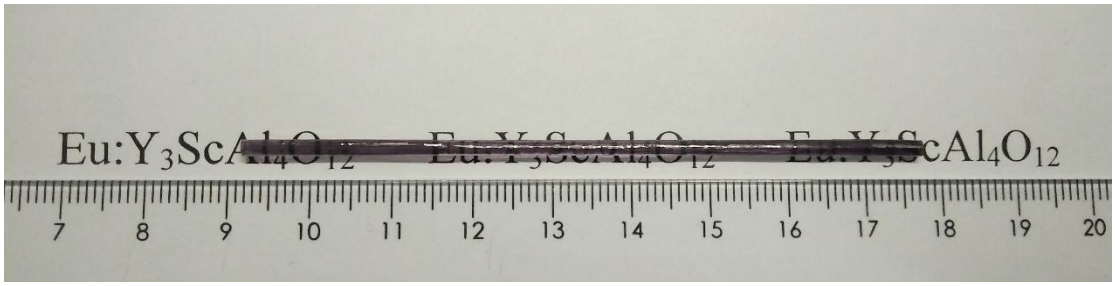

(b)

Fig. 1. Photographs of the as-grown Eu:YAG (a) and Eu:$Y_3ScAl_4O_{12}$ (b) crystals.

3.2 Crystal structure

The corresponding XRD patterns are shown in Fig. 2. All the diffraction peaks matched well with the standard card of YAG (PDF#88-2048), and no impurity peaks were found in the patterns, indicating that the Eu^{3+} ions were well diffused in the host lattices and did not change the crystalline structure. The Eu^{3+} is expected to substitute Y^{3+} into the distorted dodecahedral site and to be coordinated to eight O^{2-} ions because of their comparable ionic size. The calculated cell parameters of Eu^{3+}-doped YAG and $Y_3ScAl_4O_{12}$ single crystals were a=11.957 Å, and a= 12.053 Å, respectively. The increase in the lattice parameter of YSAG is

attributed to the larger ionic radius of Sc^{3+} (0.75 Å) compared to Al^{3+} ions (0.39 Å).

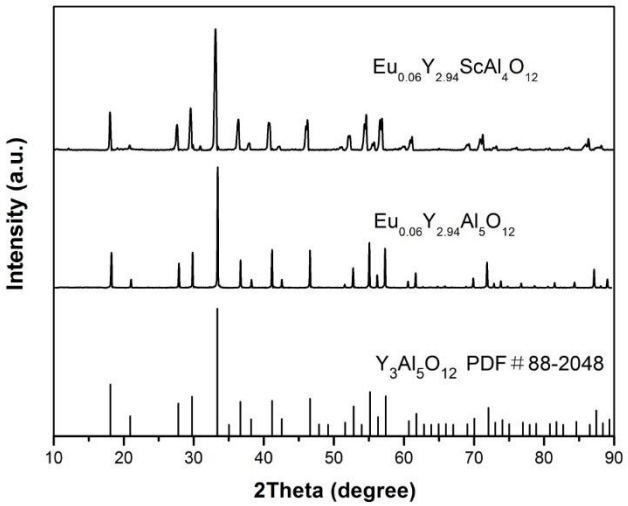

Fig. 2. XRD patterns of Eu:YAG and Eu:$Y_3ScAl_4O_{12}$ crystals with a standard pattern of YAG (PDF#88-2048).

The Raman spectra of Eu^{3+}-doped YAG and $Y_3ScAl_4O_{12}$ single crystals are shown in Fig. 3. The Raman spectra are in consistent with the spectra of Yb:YAG [24] and Nd:$Y_3Sc_2Al_3O_{12}$ crystal [25]. The Raman peaks position and intensity are changed after the introduction of Sc^{3+} ions in YAG crystal. However, no distinct changes in the modes are observed, which suggests that the crystal structure remains the same. Additionally, the maximum phonon energy of Eu:$Y_3ScAl_4O_{12}$ was determined to be 768 cm^{-1} from the Raman spectra, which is lower than that of Eu:YAG (780 cm^{-1}).

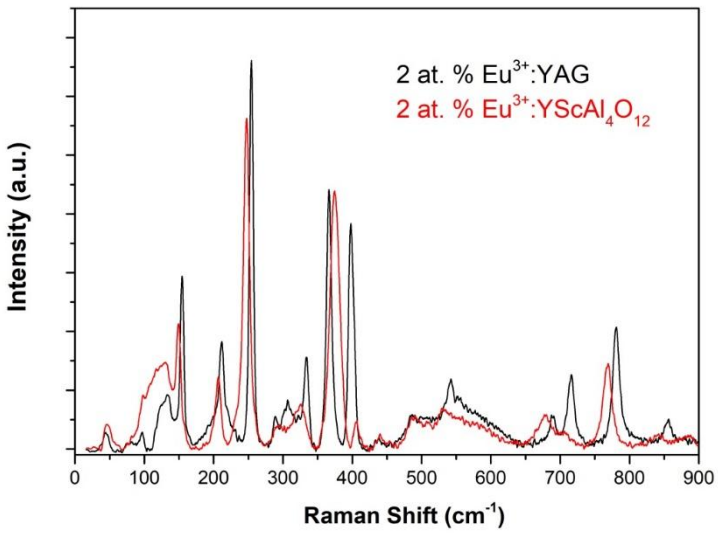

Fig. 3.The Raman spectra of Eu:YAG and Eu:$Y_3ScAl_4O_{12}$ crystals.

3.3 Optical characterization

The room temperature absorption spectra of Eu^{3+}-doped YAG and $Y_3ScAl_4O_{12}$ crystals in the range from 300 to 450 nm are shown in Fig. 4. The corresponding transitions from the $^7F_0$, $^7F_1$ ground state to excited state were assigned and marked. The absorption spectra of Eu:YAG and Eu:$Y_3ScAl_4O_{12}$ crystals are dominated by a strong line occurring at 395 nm, corresponding to the $^7F_0 \rightarrow {}^5L_6$ transition, matching well with the emission of commercial ultraviolet laser diodes. In addition, the absorption coefficient at 395 nm of Eu:YAG and Eu:$Y_3ScAl_4O_{12}$ was calculated to be 1.07 and 1.12 cm^{-1}, and the full width at half maximum (FWHM) of absorption band at 395 nm was calculated to be 1.89 and 2.21 nm respectively, which is higher than that of Eu:$CaGdAlO_4$ (1.62 nm) [12], but smaller than that of Eu:$Bi_4Ge_3O_{12}$ (3.1 nm) [15].

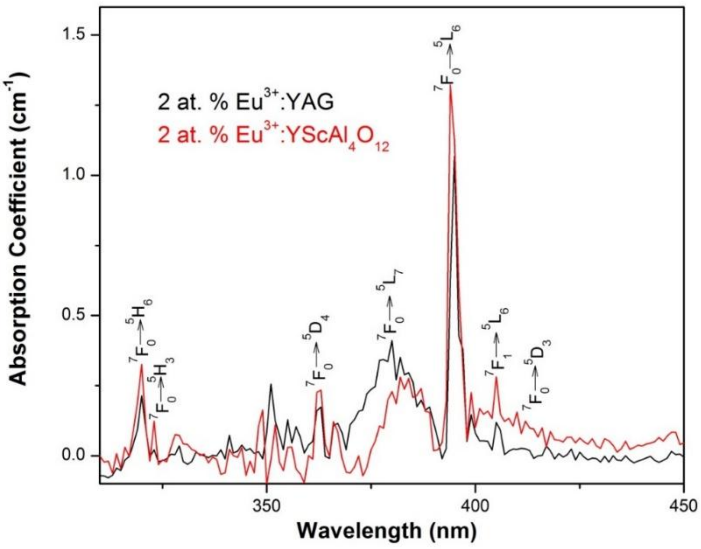

Fig. 4. The absorption spectra of Eu:YAG and Eu:$Y_3ScAl_4O_{12}$ crystals.

The fluorescence spectra of Eu:YAG and Eu:$Y_3ScAl_4O_{12}$ crystals in the wavelength range of 550-770 nm excited by 394 nm at room temperature are shown in Fig. 5. It's clear that emission bands centered around 591 nm, 610 nm, 650 nm, 710 nm, 743 nm are corresponding to transitions from $^5D_0$ excited level to $^7F_1$, $^7F_2$, $^7F_3$, $^7F_4$ and $^7F_5$ energy level, respectively, and these peaks split into some stark components. The emission in the range (580-600 nm) of Eu^{3+} due to the magnetic dipole transition of $^5D_0 \rightarrow {}^7F_1$ is not affected much by the site symmetry, because they are partly allowed, while the red emission (605-630 nm) due to the electric dipole transition of $^5D_0 \rightarrow {}^7F_2$ is sensitively affected by the site symmetry of Eu^{3+}.In Eu:$CaGdAlO_4$ crystal, the emission of $^5D_0 \rightarrow {}^7F_2$ transition is dominant because Eu^{3+} ions are located at a non-inversion symmetry position in $CaGdAlO_4$ crystal [12]. However, in Eu:YAG and Eu:$Y_3ScAl_4O_{12}$ crystals, Eu^{3+} ions occupy a site with inversion symmetry, which induces the relative weak emission of the $^5D_0 \rightarrow {}^7F_2$ transition at 610 nm. Furthermore, the ratio between the integrated intensity of $^5D_0 \rightarrow {}^7F_2$ and $^5D_0 \rightarrow {}^7F_1$ transitions ($^5D_0 \rightarrow {}^7F_2/{}^5D_0 \rightarrow {}^7F_1$) is called asymmetric ratio (R_{21}), which gives information about the surrounding and environmental changes around the Eu^{3+} ions. The higher the asymmetric ratio is, the more apart from a centrosymmetric geometry luminescent center is located [26]. The asymmetric ratio R_{21} of Eu:YAG and Eu:$Y_3ScAl_4O_{12}$ was calculated to be 0.49 and 0.48, which is much higher than that of Eu-doped

SnO_2 xerogels with low concentration (0.01 [27]), but smaller than that of $Y_{0.7}BO_3:Eu_{0.3}^{3+}@SiO_2$ nanophosphors (6.71 [28]), Eu:YAG microcrystals (1.0 [29]) and Eu:YAG nanocrystals (average value 0.75 [29]). The observed difference can be explained with more symmetric local environment in Eu:YAG monocrystals compared with Eu:YAG nanocrystals and microcrystals.

The intense emission of the $^5D_0 \rightarrow {}^7F_4$ transition at 710 nm suggests that Eu:YAG and Eu:$Y_3ScAl_4O_{12}$ crystals have potential application in red emission. Besides, The full width at half maximum (FWHM) of emission band at 710 nm was calculated to be 2.03 and 3.19 nm for Eu:YAG and Eu:$Y_3ScAl_4O_{12}$, respectively. It can be clearly observed that the emission bandwidth of Eu:$Y_3ScAl_4O_{12}$ crystal is significantly broader than that of Eu:YAG crystal due to the partially disordered crystalline structure in Eu:$Y_3ScAl_4O_{12}$.

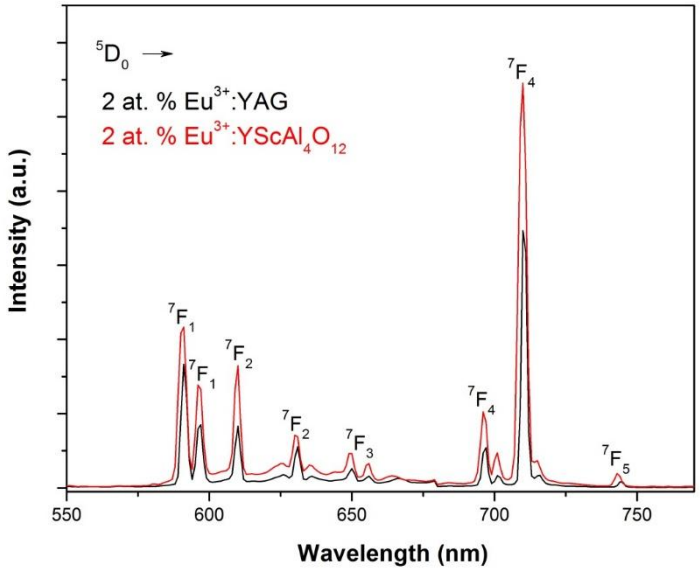

Fig. 5. The emission spectra of Eu:YAG and Eu:$Y_3ScAl_4O_{12}$crystals under 394 nm excitation

The CIE-1931 chromaticity coordinates for Eu:YAG and Eu:$Y_3ScAl_4O_{12}$ crystals were calculated and the results are illustrated in Fig. 6. The CIE coordinate of Eu:YAG and Eu:$Y_3ScAl_4O_{12}$ samples were determined to be (0.615, 0.385) and (0.635, 0.365), respectively, which was close to that of the standard value of National Television Standard Committee (NTSC) for red phosphor (0.670, 0.330).

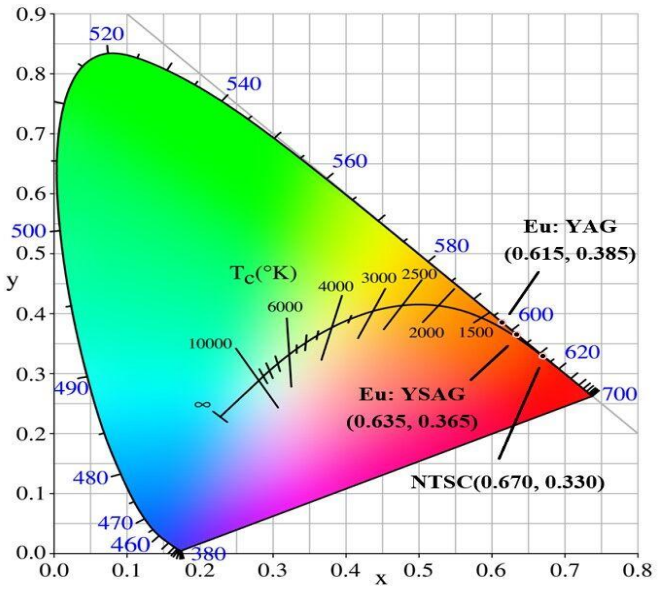

Fig. 6. CIE-1931 chromaticity diagram of Eu:YAG and Eu:$Y_3ScAl_4O_{12}$ crystals.

To further investigate the fluorescence mechanism, the room temperature fluorescence decay curves of the $^5D_0$ level excited by 394 nm were presented in Fig. 7. The measured decay curves showed a single exponential decaying behavior, and the fluorescence lifetimes of Eu:YAG and Eu:$Y_3ScAl_4O_{12}$ crystals were measured to be 3.19 and 2.97 ms, respectively, which is much longer than that of Eu:$CaGd_4O_7$ phosphors (700 μs) [30]. The incorporation of Sc^{3+} in YAG decrease the life time of the excited state ($^5D_0$) in Eu-doped YSAG around 7%. The incorporation of Sc in Eu-doped YAG can slightly affect lattice parameter inducing lattice defects, which can strongly affect the life time. The Sc environment influence the lifetime of Eu^{3+} in garnet structure. Eu:tellurite glasses (0.93 ms) [31], Eu:$CaGdAlO_4$ crystal (1.02 ms) [12] and Eu:$Bi_4Ge_3O_{12}$ crystal (1.51 ms) [15]. The result shows that Eu:YAG and Eu:$Y_3ScAl_4O_{12}$ crystals are promising candidates for red luminescent/laser materials.

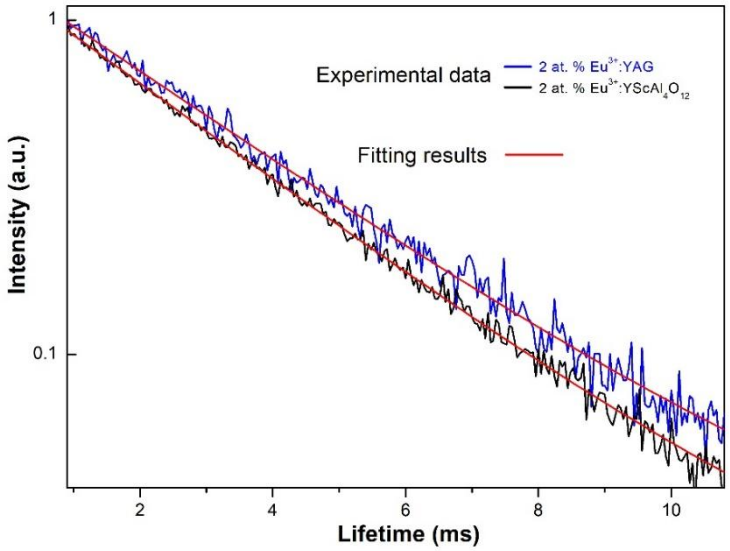

Fig. 7. Decay curves of $^5D_0$ level of Eu:YAG and Eu:$Y_3ScAl_4O_{12}$ crystals.

4. Conclusion

In this work, Eu^{3+}-doped YAG and $Y_3ScAl_4O_{12}$ single crystals have been successfully grown by the μ-PD method for the first time. The optical properties including absorption spectra, fluorescence spectra and fluorescence decay curves of Eu:YAG and Eu:$Y_3ScAl_4O_{12}$ were characterized and compared. The FWHM of absorption band at 395 nm was calculated to be 1.89 and 2.21 nm for Eu:YAG and Eu:$Y_3ScAl_4O_{12}$, respectively. The most intense red emission centered at 710 nm corresponding to the transition $^5D_0 \rightarrow {}^7F_4$, and the FWHM of emission band at 710 nm was calculated to be 2.03 and 3.19 nm for Eu:YAG and Eu:$Y_3ScAl_4O_{12}$, respectively. The lifetime of Eu:YAG and Eu:$Y_3ScAl_4O_{12}$ crystals was measured to be 3.19 and 2.97 ms, respectively. All the results show that the Eu:YAG and Eu:$Y_3ScAl_4O_{12}$ crystals are potential media for red luminescent emission.

Acknowledgements

This work is partially supported by National Key Research and Development Program of China (No. 2016YFB0701002) and National Natural Science Foundation of China (No. 61621001).

References

[1] J. Zhong, H. Gao, Y. Yuan, L. Chen, D. Chen, Z. Ji, Eu^{3+}-doped double perovskite-based

phosphor-in-glass color converter for high-power warm w-LEDs, J. Alloys Compd. 735 (2018) 2303-2310.
[2] D. Ravichandran, Rustum Roy, A.G. Chakhovskoib, C.E. Huntb, W.B. White, S. Erdei, Fabrication of $Y_3Al_5O_{12}$:Eu thin films and powders for field emission display applications, J. Lumin. 71 (1997) 291-297.
[3] S. Ruan, J. Zhou, A. Zhong, J. Duan, X. Yang, M. Su, Synthesis of $Y_3Al_5O_{12}$:Eu phosphor by sol-gel method and its luminescence behavior, J. Alloys Compd. 275–277 (1998) 72–75.
[4] P.K. Sharma, P.K. Dutta, A.C. Pandey, Performance of YAG:Eu^{3+}, YAG:Tb^{3+} and BAM:Eu^{2+} plasma display nanophosphors, J. Nanopart. Res. 14 (2012) 731.
[5] J. Su, Q. Zhang, S. Shao, W. Liu, S. Wan, S. Yin, Phase transition, structure and luminescence of Eu:YAG nanophosphors by co-precipitation method, J. Alloys Compd. 470 (2009) 306–310.
[6] G. Dong, H. Ma, Y. Liu, Z. Yang, Q. Liu, Synthesis and photoluminescence properties of the high-brightness Eu^{3+}-doped $Sr_3Bi(PO_4)_3$ phosphors, Opt. Comm. 285 (2012) 4097–4101.
[7] L. Cao, J. Liu, Z. Wu, S. Kuang, Study on the photoluminescence properties of a color-tunable $Ca_9ZnK(PO_4)_7$:Eu^{3+} phosphor, Optik 27 (2016) 4039-4042.
[8] H. Guo, X. Huang, Y. Zeng, Synthesis and photoluminescence properties of novel highly thermal-stable red-emitting $Na_3Sc_2(PO_4)_3$:Eu^{3+} phosphors for UV-excited white-light-emitting diodes, J. Alloys Compd. 741 (2018) 300-306.
[9] H. Guo, L. Sun, J. Liang, B. Li, X. Huang, High-efficiency and thermal-stable Eu^{3+}-activated $Ca_3Y(AlO)_3(BO_3)_4$ red-emitting phosphors for near-UV-excited white LEDs, J. Lumin. 205 (2019) 115-121.
[10] Q. Liu, Y. Yuan, J. Li, J. Liu, C. Hu, M. Chen, L. Lin, H. Kou, Y. Shi, W. Liu, H. Chen, Y. Pan, J. Guo, Preparation and properties of transparent Eu:YAG fluorescent ceramics with different doping concentrations, Ceram. Int. 40 (2014) 8539–8545.
[11] S. Shao, Q. Zhang, W. Liu, D. Sun, C. Gu, S. Yin, Preparation, structure and luminescence properties of nanocrystalline Eu:$Gd_3Sc_2Ga_3O_{12}$, J. Alloys Compd. 471 (2009) 263–267.
[12] R. Li, X. Xu, L. Su, Q. Sai, C. Xia, Q. Yang, J. Xu, A. Strzęp, A. Półkoszek, Crystal characterization and optical spectroscopy of Eu^{3+}-doped $CaGdAlO_4$ single crystal fabricated by the floating zone method, Chin. Opt. Lett. 14 (2) (2016) 021602.
[13] N. Ben Amar, T. Koubaa, M.A. Hassairi, I. Kbaili, M. Dammak, Optical spectroscopy of Eu^{3+} ions doped in $YAl_3(BO_3)_4$ crystal, J. Lumin. 160 (2015) 95-100
[14] V.I. Dashkevich, S.N. Bagayev, V.A. Orlovich, A.A. Bui, P.A. Loiko, K.V. Yumashev, N.V. Kuleshov, S.M. Vatnik, A.A. Pavlyuk, Quasi-continuous wave and continuous wave laser operation of Eu:$KGd(WO_4)_2$ crystal on a $^5D_0 \rightarrow {}^7F_4$ transition, Laser Phys. Lett. 12 (2015) 015006
[15] N. Li, Y. Xue, D. Wang, B. Liu, C. Guo, Q. Song, X. Xu, J. Liu, D. Li, J. Xu, Z. Xu, J. Xu, Spectroscopic properties of Eu:$Bi_4Ge_3O_{12}$ single crystal grown by the micro-pulling-down method, J. Lumin. 208 (2019) 208-212.
[16] Y. Sato, T. Taira, A. Ikesue, Spectral parameters of Nd^{3+}-ion in the polycrystalline solid-solution compared of $Y_3Al_5O_{12}$ and $Y_3Sc_2Al_3O_{12}$, Jpn. J. App. Phys. 42 (2003) 5071-5074
[17] J. Ma, J. Wang, D. Shen, A. Ikesue, D. Tang, Generation of sub-100-fs pulses from a

diode-pumped Yb:$Y_3ScAl_4O_{12}$ ceramic laser, Chin. Phys. Lett. 15 (2017) 121403
[18] C. Feng, H. Zhang, Q. Wang, J. Fang, Dual-wavelength synchronously mode-locked laser of a Nd:$Y_3ScAl_4O_{12}$ disordered crystal, Laser Phys. Lett. 14 (2017) 045804.
[19] J. Xu, Q. Song, J. Liu, S. Zhou, Y. Pan, D. Li, P. Liu, X. Xu, Y. Ding, J. Xu, K. Lebbou, Spectroscopic characteristics of Dy^{3+}-doped Y_3Al_5O12 (YAG) and $Y_3ScAl_4O_{12}$ (YSAG) garnet single crystals grown by the micro-pulling-down method, J. Lumin. 215 (2019) 116675
[20] Y. Xue, N. Li, D. Wang, Q. Wang, B. Liu, Q. Song, D. Li, X. Xu, H. Gu, Z. Qin, G. Xie, Z. Wang, J. Xu, Spectroscopic and laser properties of Tm:CNGG crystals grown by the micro-pulling-down method, J. Lumin. 23 (2019) 36-39
[21] Q. Song, X. Xu, Z. Zhou, B. Xu, D. Li, P. Liu, J. Xu, K. Lebbou, Laser operation in a Tm:LuAG crystal grown by the micro-pulling-down technique, IEEE Photon. Tech. Lett. 30 (2018) 1913-1916
[22] Q. Song, X. Xu, J. Liu, X. Bu, D. Li, P. Liu, Y. Wang, J. Xu, K. Lebbou, Structure and white LED properties of Ce-doped YAG-Al_2O_3 eutectics grown by the micro-pulling-down method. CrystEngComm, 21 (2019) 4545-4550
[23] J. Wang, Q. Song, Y. Sun, Y. Zhao, W. Zhou, D. Li, X. Xu, C. Shen, W. Yao, L. Wang, J. Xu, D. Shen, High-performance Ho:YAG single-crystal fiber laser in-band pumped by a Tm-doped all-fiber laser, Opt. Lett. 44 (2019) 455-458
[24] Y.F. Chen, P.K. Lim, S.J. Lim, Y.J. Yang, L.J. Hu, H.P. Chiang, W.S. Tse, Raman scattering investigation of Yb:YAG crystals grown by Czochralski method, J. Raman Spectrosc. 34 (2003) 882-885
[25] S. Ding, H. Wang, J. Luo, W. Liu, Y. Ma, Q. Zhang, 1 micrometer high-efficient radiation resistant laser crystal: Nd:YSAG, J. Lumin. 214 (2019) 116596
[26] E.W.J.L. Ooman, A.M.A. van Dongen, Europium (III) in oxide glasses: Dependence of the emission spectrum upon glass composition, J. Non Cryst. Solids 111(1989) 205-213
[27] E.A. Morais, L.V.A. Scalvi, A. Tabata, J..B.B. De Oliveira, S.J.L. Ribeiro, Photoluminescence of Eu^{3+} ion in SnO_2 obtained by sol–gel, J. Mater Sci. 43 (2008) 345-349.
[28] U. Rambabu, S.D. Han, Luminescence optimization with superior asymmetric ratio (red/orange) and color purity of MBO_3:Eu^{3+}@SiO_2 (M = Y, Gd and Al) nano down-conversion phosphors, RSC Adv. 3 (2013) 1368-1379.
[29] I.E. Kolesnikov, A.V. Povolotskiy, D.V. Mamonova, E.Yu. Kolesnikov, A.V. Kurochkin, E. Lahderanta, M.D. Mikhailov, Asymmetry ratio as a parameter of Eu^{3+} local environment in phosphors, J. Rare Earth. 36 (2018) 474-481.
[30] E. Pavitra, G. Seeta Rama Raju, Jin Young Park, Yeong Hwan Ko, Jae Su Yu, Synthesis and luminescent properties of novel red-emitting $CaGd_4O_7$:Eu^{3+} nanocrystalline phosphors, J. Alloys Compd. 553 (2013) 291–298.
[31] W. Stambouli, H. Elhouichet, B. Gelloz, M. Ferid, Optical and spectroscopic properties of Eu-doped tellurite glasses and glass ceramics, J. Lumin. 138 (2013) 201–208.